Fault-Tolerant Electric Actuator for Heavy Unmanned Aerial Vehicles Using a Harmonic Drive

Mohamed A.A. Ismail
Interdisciplinary Research Center for Aviation and Space Exploration, Aerospace Engineering Department,
King Fahd University of Petroleum & Minerals (KFUPM)
Dhahran 31261, Saudi Arabia
Mohamed.Ismail@kfupm.edu.sa

Abstract— **Heavy unmanned aerial vehicles (UAVs), which have a maximum takeoff weight greater than 25 kg, are driving future urban air mobility, wherein high levels of safety and reliability must be demonstrated. The flight controls of heavy UAVs are based on electromechanical actuators (EMAs), which, according to recent certification requirements, should have fault-tolerant features. This study presents the experimental testing of a novel fault-tolerant EMA architecture employing a dual coaxial electric motor, a harmonic drive gear connected to the flight control, health monitoring, and reconfiguration unit. The harmonic drive mechanism is used as a conventional gear and to measure the aerodynamic load of the flight control, thanks to its internal elasticity, without using loadcells or additional sensors. The aerodynamic load data are vital for detecting emerging faults in-flight with extreme transient operating conditions. The fault-tolerant architecture has been experimentally validated using the actuator requirements and flight data from the Automated Low Altitude Air Delivery project: a heavy UAV developed by the German Aerospace Center.**

***Keywords*— certified UAVs, fault injection, model-based fault detection, harmonic drive actuator**

I. INTRODUCTION

The growing use of heavy unmanned aerial vehicles (UAVs) in civilian applications necessitates enhanced airworthiness standards, particularly for safety-critical systems, such as the flight control electromechanical actuators (EMAs) of heavy UAVs. While manned aircraft benefit from stringent certification, ensuring high reliability, UAVs without fault-tolerant features suffer a loss rate that is tenfold higher [1]. To address this, civil aviation authorities are pushing for fault-tolerant EMA architectures akin to those in manned aviation, especially for systems that require uninterrupted operation after a failure (e.g., primary flight controls) [2].

According to the Federal Aviation Administration, large or heavy UAVs are defined as those with a maximum gross operating weight (MGOW) of 25 kg or more [3]. Heavy UAVs cannot operate under Part 107 regulations for small UAVs. The Automated Low Altitude Air Delivery (ALAADy) UAV in Fig. 1, developed by the German Aerospace Center (DLR), is an example of the future concept of delivering freight by heavy gyroplane UAVs with an MGOW of 500 kg [4].

The development of fault-tolerant EMAs has been discussed in many studies based on improvements in the health monitoring methods [5]–[7] or electromechanical design features of the actuator [8]. Examples of model-based approaches are examined in a study [5], wherein the simulated annealing algorithm for friction and backlash detection is utilized.

Additionally, another study [6] uses the monitoring of the actuator for detecting actuator degradation. However, the health monitoring methods in [5] and [6] rely on controlled excitation signals or simplified dynamic models. Conversely, data-based methods are examined in a study [7] for instantaneous efficiency calculations using the current and torque measurements of the actuator, but it lacks robustness under transient loads. A further study [8] uses a parallel active–active EMA design with loadcells to monitor and compensate for transient load disturbances in detection performance. Nevertheless, integrating loadcells means additional cost and reliability concerns owing to their relatively limited service life.

A critical gap across these studies is the handling of actuator load data: Prior work ignores load data [9], uses multiple load sensors [8], or conducts monitoring only under no-load conditions [5]. Additionally, health functions often analyze speed or load independently, despite both being essential for accurate fault diagnosis. This study presents experimental testing for a fault-tolerant EMA prototype employing redundancies and sensorless aerodynamic load estimation to reduce false diagnosis rates during transient in-flight conditions without using additional sensors. The theoretical design of the actuator and the numerical simulation have previously been published in [11].

This paper ~~has been~~ is organized into three sections. The fault-tolerant actuation architecture is described in Section 2, and the overall fault-tolerant performance is evaluated in Section 3.

Fig. 1. Example of a heavy UAV: DLR ALAADy [4]

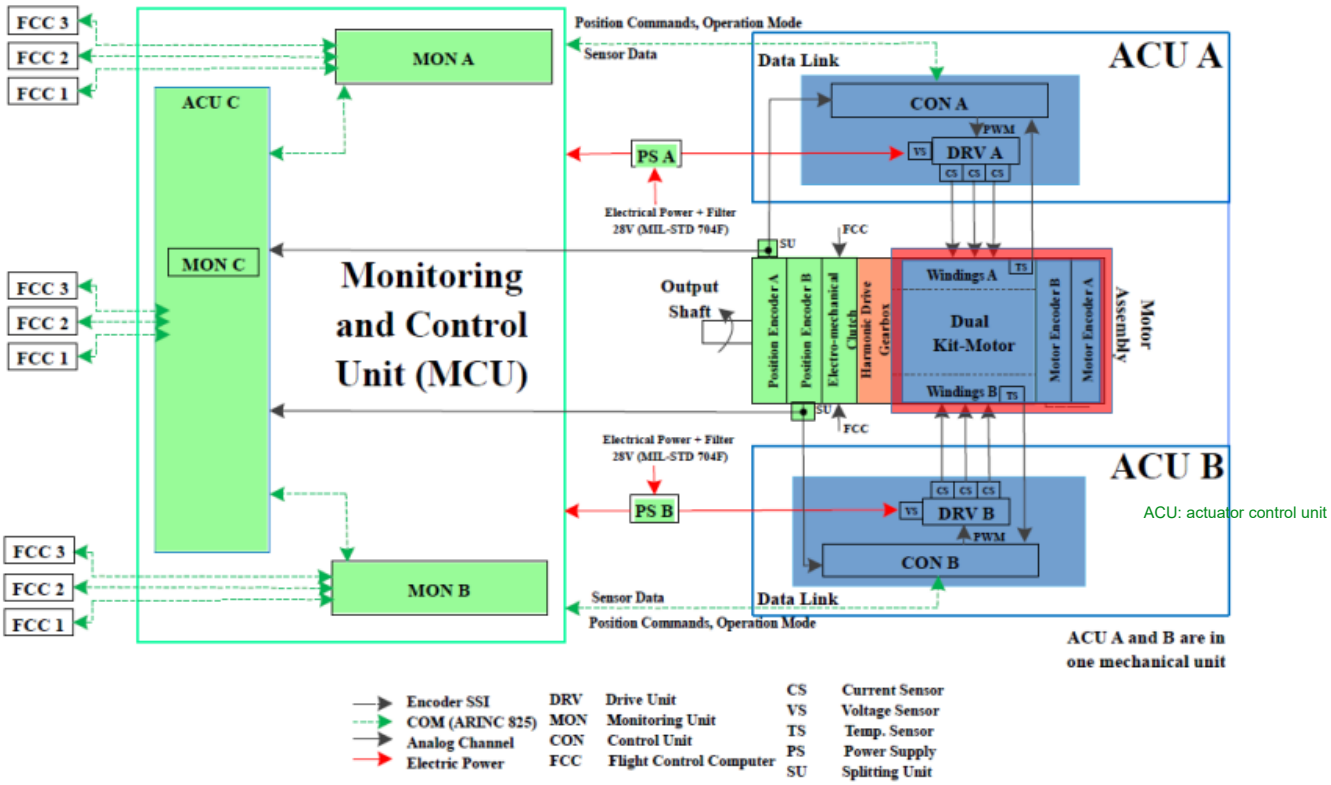

Fig. 2. Fault folerant actuation architecture

II. Fault-Tolerant Architecture

A. General Overview

The fault-tolerant EMA design (Fig. 2) employs a segregated architecture for electrical and electronic components, which are isolated to enhance system resilience. This configuration includes independent actuator control units, each of which houses separate controller (CON) and monitoring (MON) modules. The dual-channel setup ensures full isolation, with each channel powered by its own distinct supply and controlling module. Separate motors and positional encoders are integrated into every channel for localized operation. The mechanical load is managed through a harmonic drive gearbox, which directs force to a unified output mechanism. The electric motor consists of two independent coaxial modules of a three-phase reluctance motor. The motor design achieves a high power-to-weight ratio and low drag torque in the event of short-circuit faults compared to conventional permanent magnet motors. The fault-tolerant system has three operating modes: nominal, fail operational, and fail safe. Nominal mode, or active–active mode, means that the full EMA components are working normally. Fail operational, or passive–active, mode means that one actuator channel is switched off and the actuator is active with only one channel. In fail safe mode, the actuator is switched off completely. A detailed study of the electrical motor design of this architecture has been published in [10]. Coaxial modules eliminate the need for additional gearboxes to drive two rotors and minimize the risk of the actuator jamming. Three flight control computers (FCCs) are considered to maintain full operating conditions after a total failure of one FCC channel. The FCC channels are fed to individual MONs, where triple internal crossvoting is performed. Two CONs are provided to control two independent three-phase modules in an active–active configuration. Triple MONs are used to monitor individual CON units (MON1, MON2) and the mutual characteristics between active CONs to avoid any possible force fighting.

B. Sensorless Load Estimation Using a Harmonic Drive

The basic HD assembly consists of the wave generator (WG), the FS, and the circular spline (CS), as shown in Fig. 3. The WG is connected to the input shaft of the actuator motor side. The FS is attached to the flight controls. The torque estimation methods for HDs are typically based on monitoring torsion between WG and FS where CS is fixed. However, a study using methods for real industrial applications showed many limitations [11].

Fig. 3. Basic HD gear assembly

Torque estimation needs high computational resources, and the elasticity of HD is exposed to service aging. There must also be numerous calibrations. Here, the fault-tolerant architecture is based on a torque estimation method that is grounded in the structural damping of HD rather than its elasticity. The structural damping uses the torsional rate of HD rather than the static torsion in most of the literature. A detailed investigation of this torque estimation method is furnished in [11].

C. *Health Monitoring System Design*

The health monitoring system of this fault-tolerant architecture has been discussed in detail in a previous publication [11]. Here, a brief description is furnished. It consists of three monitoring units—MON A, MON B, and MON C—as shown in Fig. 2. MONs A and B are designed to perform equivalent monitoring tasks within their respective local actuation channels or lanes (Lanes A and B), focusing on identifying faults within their own lanes. In contrast, MON C specializes in detecting cross-lane faults (e.g., torque conflicts between Lanes A and B caused by sensor or communication errors). Open loop monitors (OLMs) evaluate the actuator's output shaft position-tracking accuracy. Each lane (Lanes A and B) has its own OLM—OLMA and OLMB—which employ a simplified single-input, single-output dynamic model (Gp) to represent ideal tracking behavior. These monitors independently measure the actuator's output position (θmes), using position encoders that are specific to their assigned lanes. Inner loop monitors (ILMs), or first-order tracking monitors, assess speed-tracking performance in individual lanes. Prior studies [8], [9] explored basic ILMs for EMAs to detect electrical/mechanical faults but did not account for actuator load effects. This work advances ILM designs by integrating direct compensation for actuator load, enhancing their diagnostic capability.

III. Experimental Testing

Selected performance experiments are reported here to show compliance with the actuator design requirements for the ALAADy UAV, as listed in Table 1.

Table 1: Performance requirements for EMAs [4]

Flight Control	EMA Requirements
Pitch and roll actuator	Force: 500 N Travel: 100 mm Speed: 80 mm/s Bandwidth*: 2 Hz
Rudder actuator	Torque: 30 Nm Travel: ±50° Speed: 65 °/s Bandwidth*: 2 Hz

* Bandwidth at 5 mm or 5° amplitude

A. *Test Setup*

The experimental verification of the actuator design and the fault-tolerant performance have been carried out on a special test rig for flight control EMAs at the DLR Institute of Flight systems. As shown in Fig. 4, the testbed consists of a real-time control unit based on a dSPACE platform, a load unit for generating realistic aerodynamic loads on the actuator and the fault-tolerant EMA to be tested. The test setup is also a fault injection unit controlled by dSPACE, as shown in Fig. 5. The fault-tolerant control algorithms are implemented as a SIMULINK model and compiled and downloaded to a real-time dSPACE platform. The trajectory of the reference motion and the injected faults are sent to the dSPACE interface (Control Desk) in real time with a sampling rate of 1 kHz. Two groups of tests are conducted on the test bench: nominal and fault-tolerant performance tests.

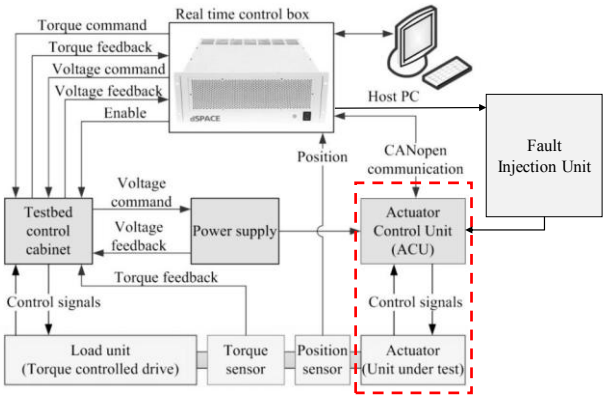

Fig. 4. Functional diagram for EMA actuator testbed

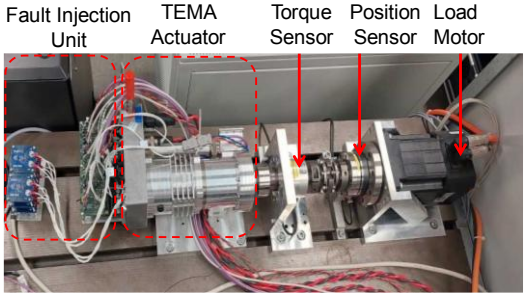

Fig. 5. The actuator prototype

B. *Nominal Performance Testing*

The objective of the nominal performance tests is to evaluate the actuator performance for tracking the reference motion trajectory according to the requirements. These tests include position-tracking tests for a step input (Fig. 6) and a sinusoidal input (Fig. 7) profile. For the applicable external load range, the actuator can follow the reference trajectory with a steady-state error of less than 0.1° and an overshoot of less than 5%. In addition, several bandwidth tests were performed to measure how fast the actuator can follow rapid reference signals. As shown in Figs. 8–9, the actuator achieves a significantly higher bandwidth than the required 3 Hz for both active–passive and active–active operation modes. The 3 Hz bandwidth is an essential requirement for the ALAADy UAV use case.

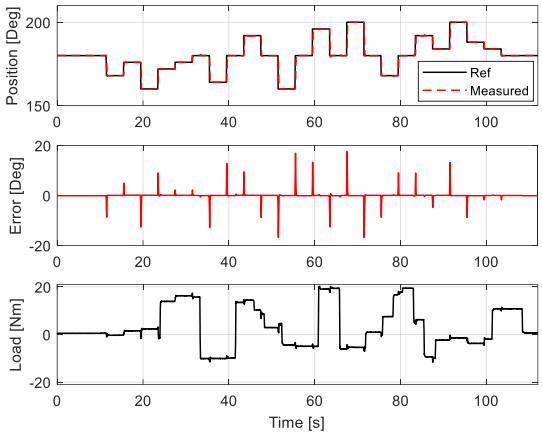

Fig. 6. Position tracking for a step motion profile

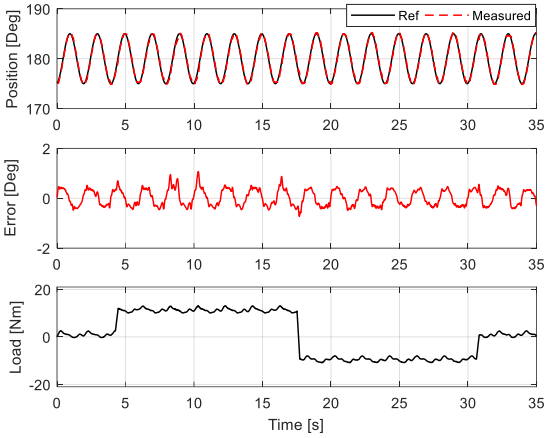

Fig. 7. Position tracking for a sinusoidal (0.5 Hz) motion profile

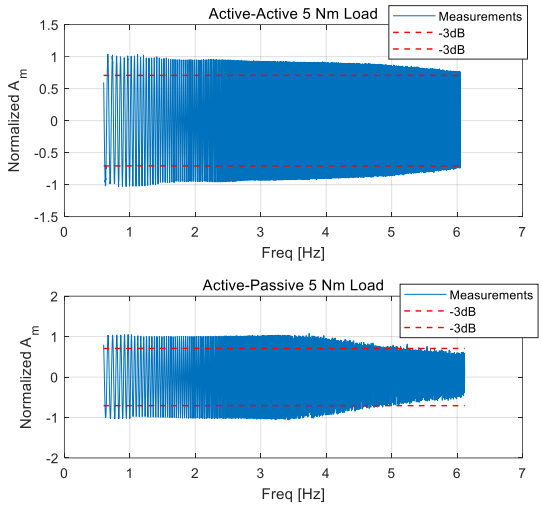

Fig. 8. –3dB bandwidth at different load levels (Am = 5º) for active–active and active–passive modes

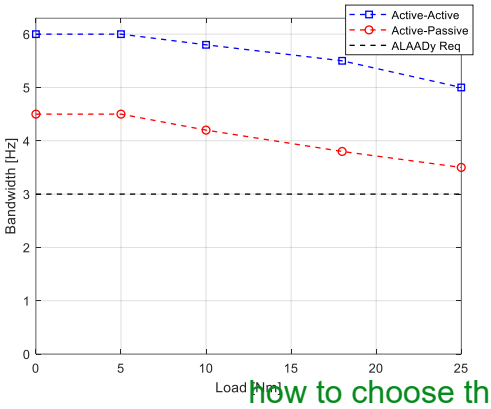

how to choose the treshold??

Fig. 9. Actuator bandwidth at different load levels (Am = 5º)

C. *Fault-Tolerant Performance Testing*

Fault tolerance tests are performed for sensor and electrical faults. Sensor faults include the loss of a position sensor or Hall sensor during a normal flight. Fig. 10 presents a case study in which the position sensor of Lane A is suddenly shut down by the fault injection unit. The expected position of the actuator is continuously estimated by the OLM and compared with the actual position of the encoders. Once an encoder fault occurs, the OLM error residual increases over time. If the residual is higher than the threshold (fault latency threshold) for a certain time interval, the controller shuts down the defective lane. Here, the time difference between the fault injection and detection is only 0.2 seconds. The actuator is now in fail operational mode or passive–active configuration. If a second fault is injected, such as the Hall sensor loss in Fig. 11, an abnormal residual of the ILM is detected by the actuator controller and shuts down the defective lane.

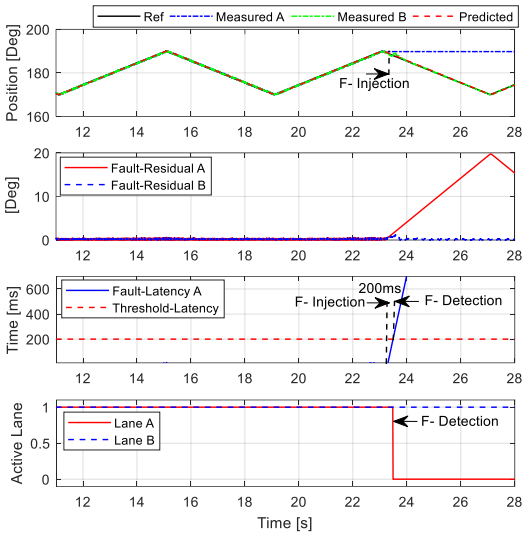

Fig. 10. Loss of encoder sensor signal—Lane A

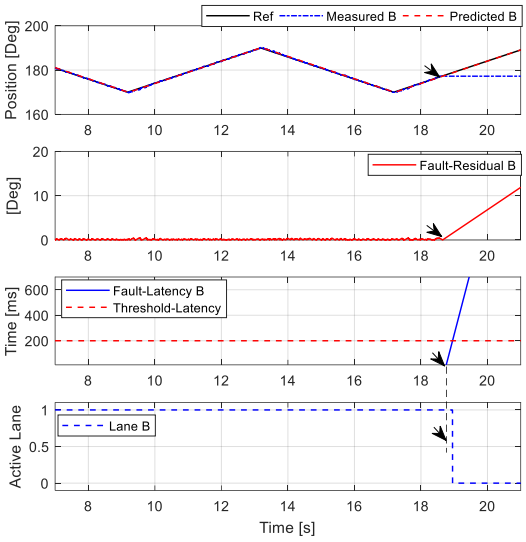

Fig. 11. Loss of Hall sensor signal—Lane B

IV. Conclusion

This study presents the experimental testing for a fault-tolerant EMA prototype employing redundancies and sensorless aerodynamic load estimation to reduce false diagnosis rates during transient in-flight conditions without using additional sensors. These results collectively affirm the actuator's robustness, precision, and fault-tolerant design. The integration of advanced monitoring algorithms (OLM and ILM) with a redundant control architecture ensures compliance with safety-critical aviation standards. The system's ability to exceed bandwidth requirements while maintaining 0.1° tracking errors and 5% overshoots positions it as a reliable solution for UAV applications demanding high performance under operational uncertainties. Moreover, the sub-second fault detection and reconfiguration capabilities enhance operational safety, making the actuator suitable for scenarios in which system failures could lead to mission-critical risks. In summary, the actuator fulfills and surpasses the ALAADy UAV's technical prerequisites, offering a resilient, high-performance solution for advanced aerial systems.

V. Acknowledgment

This article is sponsored by project no. INAE2404 funded by the Interdisciplinary Research Center for Aviation and Space Exploration, King Fahd University of Petroleum & Minerals (KFUPM). The research data was conducted within TEMA-UAV project (2019-2022) at DLR (German Aerospace Center) through the German Aerospace Research Program (Lufo V-3).

References

[1] I. Sadeghzadeh and Y. A. Zhang, "Review on fault-tolerant control for unmanned aerial vehicles (UAVs)," *Infotech@Aerospace Conf.* St. Louis, MO, USA, Mar. 29–31, 2011.

[2] C. Bosch, M. A. Ismail, S. Wiedemann, and M. Hajek. *Towards Certifiable Fault-Tolerant Actuation Architectures for UAVs: Advances in Condition Monitoring and Structural Health Monitoring*. Lecture Notes in Mechanical Engineering. Singapore: Springer, 2021, pp. 355–364.

[3] US Federal Aviation Administration. https://www.faa.gov/air_traffic/publications/atpubs/aim_html/chap11_section_3.html. (accessed April. 5, 2025).

[4] A. Bierig, S. Lorenz, M. Rahm, and P. Gallun, "Design considerations and test of the flight control actuators for a demonstrator for an unmanned freight transportation aircraft," *Recent Advances in Aerospace Actuation Systems and Components Conf.* Toulouse, France. May 2018.

[5] M. D. L. Dalla Vedova, D. Lauria, P. Maggiore, and N. Pace. "Linear electromechanical actuators affected by mechanical backlash: A fault identification method based on simulated annealing algorithm," *WSEAS Transactions on Systems*, pp. 268–276, 2015.

[6] G. Swerdon, M. Watson, S. Bharadwaj, C. S. Byington, M. Smith, K. Goebel, and E. Balaban, "A system engineering approach to electro-mechanical actuator diagnostic and prognostic development," *Machinery Failure Prevention Technology (MFPT) Conf.* Dublin, Ireland, June 2009, pp. 23–25.

[7] M. Todeschi and L. Baxerres, "Health monitoring for the flight control EMAs," *IFAC-PapersOnLine*, vol. 48, no. 21, pp. 186–193, 2015.

[8] D. Arriola and F. Thielecke, "Model-based design and experimental verification of a monitoring concept for an active–active electromechanical aileron actuation system," *Mechanical Systems and Signal Processing*, vol. 94, pp. 322–345, 2017.

[9] D. Rito and F. Schettini, "Health monitoring of electromechanical flight actuators via position-tracking predictive models," *Advances in Mechanical Engineering*, vol. 10, no. 4, pp. 1–12, 2018.

[10] M. A. Ismail, S. Wiedemann, C. Bosch, and C. Stuckmann, "Design and evaluation of fault-tolerant electro-mechanical actuators for flight controls of unmanned aerial vehicles," *Actuators*, vol. 10, no. 8, p. 175, Jul. 2021.

[11] M. A. Ismail, J. Windelberg, and G. Liu, "Simplified sensorless torque estimation method for harmonic drive based electro-mechanical actuator," *IEEE Robotics and Automation Letters*, vol. 6, no. 2, pp. 835–840, 2021.